# Accepted Manuscript

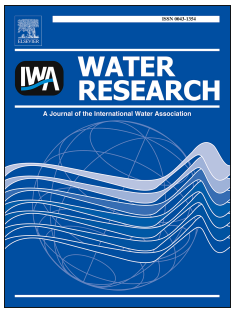


A systematic study of multiple minerals precipitation modelling in wastewater treatment

Christian Kazadi Mbamba, Stephan Tait, Xavier Flores-Alsina, Damien J. Batstone

PII: S0043-1354(15)30192-5

DOI: 10.1016/j.watres.2015.08.041

Reference: WR 11488

To appear in: *Water Research*

Received Date: 12 March 2015

Revised Date: 23 July 2015

Accepted Date: 22 August 2015

Please cite this article as: Mbamba, C.K., Tait, S., Flores-Alsina, X., Batstone, D.J., A systematic study of multiple minerals precipitation modelling in wastewater treatment, *Water Research* (2015), doi: 10.1016/j.watres.2015.08.041.

# A systematic study of multiple minerals precipitation modelling in wastewater treatment

**Christian Kazadi Mbamba [a,*], Stephan Tait [a], Xavier Flores-Alsina [b], Damien J. Batstone [a]**

[a] Advanced Water Management Centre, The University of Queensland, St Lucia, Brisbane, QLD 4072, Australia

[b] CAPEC-PROCESS, Department of Chemical and Biochemical Engineering, Technical University of Denmark, Building 229, DK-2800 Lyngby, Denmark.

[*]Corresponding author. Tel.: +61 73 346 7216; fax: +61 73 365 4726; email: c.kazadimbamba@awmc.uq.edu.au

## ABSTRACT

Mineral solids precipitation is important in wastewater treatment. However approaches to minerals precipitation modelling are varied, often empirical, and mostly focused on single precipitate classes. A common approach, applicable to multi-species precipitates, is needed to integrate into existing wastewater treatment models. The present study systematically tested a semi-mechanistic modelling approach, using various experimental platforms with multiple minerals precipitation. Experiments included dynamic titration with addition of sodium hydroxide to synthetic wastewater, and aeration to progressively increase pH and induce precipitation in real piggery digestate and sewage sludge digestate. The model approach consisted of an equilibrium part for aqueous phase reactions and a kinetic part for minerals precipitation. The model was fitted to dissolved calcium, magnesium, total inorganic carbon and phosphate. Results indicated that precipitation was dominated by the mineral struvite,

forming together with varied and minor amounts of calcium phosphate and calcium carbonate. The model approach was noted to have the advantage of requiring a minimal number of fitted parameters, so the model was readily identifiable. Kinetic rate coefficients, which were statistically fitted, were generally in the range 0.35-11.6 $h^{-1}$ with confidence intervals of 10-80% relative. Confidence regions for the kinetic rate coefficients were often asymmetric with model-data residuals increasing more gradually with larger coefficient values. This suggests that a large kinetic coefficient could be used when actual measured data is lacking for a particular precipitant-matrix combination. Correlation between the kinetic rate coefficients of different minerals was low, indicating that parameter values for individual minerals could be independently fitted (keeping all other model parameters constant). Implementation was therefore relatively flexible, and would be readily expandable to include other minerals.

Keywords: Physico-chemical modelling, precipitation, struvite, kinetics, equilibrium, parameter estimation

## 1. Introduction

Modelling of physico-chemical processes in wastewater treatment systems has received substantial attention in recent years, due to the increased use of minerals precipitation, and the interest to better understand, manipulate and optimize minerals precipitation performance via mathematical modelling (Batstone et al. 2006, Batstone et al. 2012). Minerals precipitation heavily interacts with other physico-chemical reactions (Stumm and Morgan 1996, Morel and Hering 1993) and influences wastewater composition dynamically by sequestering solubles (Le Corre et al. 2009). In addition, minerals precipitation causes inorganic scale formation

which is a well-known maintenance problem (Doyle and Parsons 2002) and can negatively impact on biological processes occurring in wastewater treatment, such as in anaerobic sludge blanket reactors treating pulp and paper wastewater (van Langerak et al. 2000, Batstone and Keller 2003). In contrast, precipitation can also have positive impacts in wastewater treatment, for example sulphide precipitation which limits the toxicant dissolved sulphide in anaerobic digesters (Chen et al. 2008) or with nutrient recovery (Mehta and Batstone 2013). Unfortunately, the description of multiple minerals precipitation in current industry-wide process simulation models (such as ASM2d and ADM1, Henze et al. 2000, Batstone et al. 2002) is empirical, incomplete or inadequate (Henze et al. 2000, Batstone 2006). This is at least partly due to a general focus on biology, but also due to a lack of robust (numerically stable) approaches to model pH, soluble ion pairing and minerals precipitation together with biological processes (Batstone et al. 2012).

A large number of potential precipitants can form during wastewater treatment. Key precipitating species in wastewater treatment include carbonates and phosphates of calcium and magnesium (Musvoto et al. 2000, van Rensburg et al. 2003, Barat et al. 2011). Some of the minerals are also capable of forming a variety of different minerals, including amorphous and crystal polymorphs (Kralj et al. 1997, Meyer and Weatherall 1982, Brečević and Nielsen 1989). This is consistent with the Ostwald rule of stages, which stipulates that the formation of a more stable phase can be preceded by the preferential formation of one or more thermodynamically less stable precursor phases (Mullin 2001). A multi-sequential-step approach has been previously used for modelling of minerals precipitation (Barat et al. 2011, Kralj et al. 1997), whereby the rate kinetics of one more stable mineral is assumed to be dependent on the concentration of another less stable precursor mineral. This modelling approach can substantially add complexity to a wastewater model due to inclusion of a multi-step process. A simpler approach (which is advocated in the present study) is parallel

precipitation modelling where minerals are assumed to form simultaneously and independently, competing for the same pool of participating ions in the aqueous phase (Musvoto et al. 2000, Ekama et al. 2006). In this case, a faster forming less thermodynamically stable mineral could re-dissolve to supply ions to a slower forming more thermodynamically stable mineral. The parallel modelling approach could also quantify the influence of precipitation rate kinetics on final mineral product mix.

A recent study (Kazadi Mbamba et al. 2015) proposed a precipitation modelling approach which was tested on calcite precipitating in synthetic aqueous solutions. This applied equilibrium-constraints for aqueous-phase reactions and a kinetic description for minerals precipitation with an *nth* order dependency on thermodynamic supersaturation. Based on observed evidence, the model also included a $1^{st}$ order effect of the amount of mineral phase present in the wastewater ($X_{cryst}$). The only contestable parameter (i.e., which required fitting) was a precipitation rate coefficient, because saturation extent was fully defined by thermodynamics. The model approach was observed to be more tolerant to a fast precipitation rate coefficient (Kazadi Mbamba et al. 2015), which implied that a modeller could select an arbitrarily high kinetic rate coefficient when process data was not available to estimate model parameters. Thus, the modelling approach of Kazadi Mbamba et al. (2015) could be well-suited to modelling multi-species systems. Each precipitation reaction would only have one fitted parameter, the kinetic rate coefficient, which could potentially be set arbitrarily high without needing sophisticated parameter estimation. However, the approach of Kazadi Mbamba et al. (2015) has not been tested for multi-species systems or real wastewater and this is the focus of the present study.

Another critical issue is the identification of model parameters. These are often determined via manual fitting (Musvoto et al. 2000, Ekama et al., 2006), which can be tedious, may be unreliable and provides little information on parameter correlation and bounds of parameter

confidence. A systematic approach is instead applied in the present paper to identify model characteristics with respect to statistically fitted precipitation rate parameters.

## 2. Materials and methods

Experiments were performed to provide robust data that reflected dynamic behaviour and allowed statistical estimation of kinetic model parameters. The experiments were performed in batch using dynamic titration or aeration to progressively increase wastewater pH and induce minerals precipitation. Measurements tracked the change in pH and dissolved calcium, magnesium, total inorganic carbon, inorganic nitrogen and phosphate, due to minerals precipitating.

### *2.1 Sample materials*

Experiments were carried out using synthetic and real wastewaters which were:

- *Synthetic wastewater:* synthetic aqueous solutions prepared as described by Kazadi Mbamba et al. (2015).
- *Piggery digestate:* effluent from a partially covered anaerobic piggery lagoon at a piggery near Grantham QLD (see Skerman and Collman (2012) for further details).
- *Sewage sludge digestate*: anaerobic digester sludge collected from a domestic wastewater treatment plant in South East Queensland, with combined primary and secondary sludge digestion.

The real wastewater samples were kept in sealed containers at ambient temperature to minimize $CO_2$ stripping and to limit inadvertent precipitation before the experiments. The

supernatants, which were used in the experiments, were decanted after the wastewater samples had settled for at least 2 days. All the samples were characterized prior to the experiments for dissolved major elements using Inductively Coupled Plasma Optical Emission Spectroscopy (ICP-OES), flow injection analysis (FIA), ion chromatography (IonC) and total carbon analysis (TCA) (see Analytical techniques).

*2.2 Apparatus*

The dynamic titration experiments used an auto-titrator (T70, Mettler-Toledo, Greifensee, Switzerland) with a pH sensor (Model DGi115-SC, Mettler-Toledo, Greifensee, Switzerland). The titration vessel used was a 1 L stirred glass crystallizer. During a titration, the test sample to which titrant was added was stirred with a 40 mm teflon-coated magnetic bar stirrer at 300 rpm. The volume of each titrant added, the pH and the temperature were recorded over time through a LabX Light Titration Software interface (Mettler-Toledo, Greifensee, Switzerland).

The aeration experiments used a crystallizer which was a 1.1 L Pyrex glass vessel and lid with open ports. The crystallizer, positioned over a magnetic stirrer plate, was stirred with a 40 mm teflon-coated magnetic bar stirrer at 350 rpm. pH change by aeration was monitored with a pH sensor (Model DGi115-SC, Mettler-Toledo, Greifensee, Switzerland), connected to the auto-titrator and recorded over time through the LabX Light software. During the aeration experiment, wastewater was aerated with a flexible polymer fine bubble air diffuser tube (Liya Aquarium “Air Curtain”). At the beginning of each aeration experiment, the air flow rate was set to a fixed value with an air flowmeter with a manual fine flow-adjustment valve (Water Key Instruments, Trevose USA).

150 *2.3 Experimental procedures*

151

152 Four experiments were performed for model analysis, classified as follows:

153 • *Experiment 1 - Continuous pH titration tests with synthetic wastewater*, to test the
154 competition of various major divalent cations with higher concentration of phosphate,
155 in the absence of inorganic carbon. The initial pH of a 1 L aliquot of test wastewater
156 was adjusted to a desired value using concentrated sodium hydroxide (NaOH) or
157 hydrochloric acid (HCl) solutions, with the amount of added acid or caustic recorded.
158 A 2M aqueous solution of NaOH (5-10 mL total) was then quantitatively added at a
159 predetermined fixed rate and pH was continuously measured. 100 $mg.L^{-1}$ of struvite
160 crystal seed (prepared as described by Mehta and Batstone 2013) was then added at a
161 time point in the experiment where the solution was estimated (using equilibrium
162 predictors) to have transitioned from undersaturated to supersaturated conditions with
163 respect to struvite.

164 • *Experiment 2 - Aeration experiments with piggery digestate and added phosphate.* To
165 raise the level of phosphate of the piggery digestate, 0.255 g of $NaH_2PO4$ was added
166 to 1000 mL of piggery digestate (increased to 65.8 mgP/L). This amended piggery
167 digestate was aerated to strip carbon dioxide ($CO_2$) to raise pH and induce
168 precipitation. pH values were continuously measured and recorded over a typical test
169 time of 24 hours.

170 • *Experiment 3 - Aeration experiments on sewage sludge digestate*. Similar to
171 experiment 2, but with the different wastewater and without added phosphate.

172 • *Experiment 4 - Aeration experiments on sewage sludge digestate at different TSS*
173 *contents.* Similar to experiment 3, but with different native TSS concentrations.
174 Settled supernatant and unsettled digestate samples were volumetrically mixed to

achieve target TSS concentrations of 1118 gTSS.m$^{-3}$, 4002 gTSS.m$^{-3}$ and 10959 gTSS.m$^{-3}$.

All the experiments were carried out at measured room temperature (20 – 25$^{o}$C). For chemical analysis in each experiment, 3 mL samples of the titration vessel contents were collected at specified time intervals, immediately filtered through 0.45 µm cut-off syringe filters (PES), diluted with deionized water to prevent post-precipitation and stored at 4$^{o}$C until analysis by ICP-OES, FIA, IonC and TCA (see directly below).

*2.4 Analytical techniques*

The major elements (Ca, Mg, Na, K) were analysed with ICP-OES (Perkin Elmer Optima Model 7300DV, Waltham, MA, USA) after nitric acid digestion. Ionic concentrations N-$NH_4^+$ and P-$PO_4^{-3}$ were quantified with a Lachat QuickChem flow injection analyser (Lachat Instruments, Loveland, CO, USA) using standard method 31-107-06-1-A. Total Inorganic Carbon (TIC) concentrations were quantified using a Total Carbon Analyser (Shimadzu TOC-L CSH Total Organic Carbon Analyser, Kyoto, Japan). Chloride, sulphide, thiosulfate, sulphite and sulphate concentrations were measured by IonC using a Dionex ICS-2000 IC System fitted with an AS50 Autosampler and AD25 Absorbance Detector (Dionex, Sunnyvle, CA). A RFIC IonPac AS18 column was used with the instrument. The sample was eluted with a KOH gradient (12 – 52 mM) and absorbance was measured at a wavelength of 230 nm. The IC analyses were performed at 35$^{o}$C. The pH in all experiments was measured with a pH sensor (Model DGi115-SC, Mettler-Toledo, Greifensee, Switzerland), and it is especially noted here that a highly precise and reliable pH sensor is essential for minerals precipitation studies. Total suspended solids (TSS) were determined as a difference between total solid

(TS) and total dissolved solid (TDS). TS was measured by evaporating and drying a wastewater sample at specified temperature (103 to 105 $^{o}$C). TDS was determined as for TS but on wastewater samples filtered through 0.45 µm cut-off syringe filters (PES).

*2.5 Physico-chemical model*

The model structure consisted of three parts;

(1) *Equilibrium part* - An algebraic equation set describing rapid aqueous phase reactions (weak acid-base and ion complexation), previously fully described by Kazadi Mbamba et al. (2015) and Solon et al. (2015).

(2) *Kinetic part* - An ordinary differential equation set describing dynamics for dissolved components, including dilution, chemical precipitation and dissolution reactions. The kinetic rate expression for precipitation/dissolution was similar to that used by Kazadi Mbamba et al. (2015), but in expanded form for multiple minerals.

(3) *Gas ($CO_2$ and $NH_3$) stripping* was described by specific volumetric mass transfer using $k_L a$ kinetics.

The implicit algebraic equation set of the Equilibrium part consisted of a reduced substituted combination of equilibrium relationships and molar contribution balances (Kazadi Mbamba et al. 2015). Thermodynamic equilibrium constants were sourced from the Visual MINTEQ database (Version 3.0, Royal Institute of Technology (KTH)) and were corrected for temperature using the van't Hoff equation as described by Kazadi Mbamba et al. (2015).

The kinetic part of the model consisted of dynamic state equations for total dissolved species and each mineral solid state ($X_{cryst}$, with units of moles.L$^{-1}$). The rate expression for minerals precipitation rate was (Kazadi Mbamba et al. 2015):

$$r_{cryst} = k_{cryst} X_{cryst} \sigma^n \quad (1)$$

where $r_{cryst}$ is the mineral precipitation rate (moles.L$^{-1}$.h$^{-1}$), $k_{cryst}$ is an empirical kinetic rate coefficient (h$^{-1}$), $X_{cryst}$ (moles.L$^{-1}$) is the concentration of precipitate at any time $t$ (a dynamic state variable), $n$ is the order of the precipitation reaction (equal to 3 for struvite and equal to 2 for other minerals) with respect to supersaturation, $\sigma$, calculated as follows for struvite as an example (Nielson, 1984):

$$\sigma = \left( \frac{Z_{(Mg^{2+})} \times Z_{(NH_4^+)} \times Z_{(PO_4^{3-})}}{K_{spStruv}} \right)^{1/3} - 1 \quad (2)$$

where $Z_{(Mg+2)}$, $Z_{(NH4+)}$ and $Z_{(PO4-3)}$ are the chemical activities of magnesium, ammonium and phosphate ions in the aqueous phase and $K_{SP,Struv}$ is the solubility product constant for pure struvite ($10^{-13.26}$, (Ohlinger et al., 1998)).

Table 1 presents the individual kinetic rate expressions for various relevant precipitation reactions. The initial conditions for the particulate mineral states (e.g. $X_{struv}$) were nominally set at a value of $10^{-5}$ Mole.L$^{-1}$ (Kazadi Mbamba et al. 2015), except in *Experiment 1* to which 100mg/L of struvite seed was added, where instead $X_{struv}$ was initially set to $10^{-3}$ Mole.L$^{-1}$.

$CO_2$ gas exchange was modelled by single-film-controlled mass transfer as follows (Batstone et al. 2002):

$$r_{CO_2\,(g)} = k_L a \left( Z_{CO_2\,(aq)} - K_H P_{CO_2\,(g)} \right) \quad (3)$$

where $k_L a$ (h$^{-1}$), $Z_{CO_2\,(aq)}$ (mole.L$^{-1}$), $K_H$ (mole.L$^{-1}$.atm$^{-1}$), $P_{CO_2\,(g)}$ (atm) are the overall film mass transfer coefficient, concentration of dissolved carbon dioxide in the liquid bulk phase at time $t$ (as calculated by the Equilibrium model part), the Henry's law constant (0.034

mole.$L^{-1}$.$atm^{-1}$) (also corrected for temperature using van't Hoff) and the partial pressure of $CO_2$ (0.00032 atm) in air being sparged, respectively. The $k_L a$ value for $CO_2$ stripping was estimated during dynamic parameter estimation. Ammonia gas exchange ($pKa$ = 9.244, $K_H$ = 58 mole.$L^{-1}$.$atm^{-1}$) was also considered in the model where relevant, using a rate expression similar to Equation 3, and recognising that ammonia gas transfer would likely be gas-film controlled (Batstone et al., 2012).

*2.6 Model implementation*

The combined differential-algebraic equation set was implemented in Matlab C-MEX files, and solved in MATLAB/SIMULINK (Version 8.1, Mathworks inc) as previously described elsewhere (Kazadi Mbamba et al. 2015, Solon et al. 2015, Flores-Alsina et al., 2015). Note that the model implementation was purposefully prepared to be modular plug-and-play and compatible with other MATLAB/SIMULINK wastewater process models such as the plant-wide Benchmark Simulation Model no. 2 (BSM2) (Gernaey et al. 2014).

*2.7. Parameter estimation*

Optimum values of kinetic coefficients $k_{cryst}$ and $k_L a$ (Equations 1 and 3) were estimated by separately fitting the dataset from each experiment, using a non-linear local optimization technique, *lsqcurvefit*, in MATLAB with the default 'trust-region-reflective' algorithm (Optimization Toolbox User's Guide Release 2014b, The MathWorks, Inc., Natick, Massachusetts, United States). Soluble concentrations of calcium, magnesium, phosphate and total inorganic carbon were all selected and used as the fitted output being simultaneously optimised. Residual sum of squares (RSS) was used as objective function ($J=RSS=\Sigma(y-\hat{y})^2$),

where $J$ is the objective function, RSS is the residual sum of squares, $y$ is the experimentally measured output and $\hat{y}$ is the simulated output. Linear estimates of confidence intervals were represented either by parameter standard error (from the Fisher information matrix), or non-linear confidence regions based on an F-test in $J$ as follows (Lobry et al. 1991):

$$J_{\text{crit}} = J_{\text{opt}} \left(1 + \frac{p}{N_{\text{data}} - p}\right) F_{(0.95,P,N_{\text{data}}-p)} \quad (4)$$

where $J_{\text{crit}}$ defines the limit of model validity, $J_{\text{opt}}$ is the optimum objective function value, $p$ is the number of fitted parameters (2 or 3, see Results), $N_{\text{data}}$ is the number of experimental data points and $F_{0.95,\text{p,ndata-p}}$ is the cumulative $F$ distribution value (computed with *finv* function in MATLAB). Parameter surfaces corresponding to $J_{\text{crit}}$ were found using a gradient search method as previously described elsewhere (Batstone et al. 2003).

### *2.8. Identifying minerals that precipitate*

Methods to identify precipitating species have included prior knowledge and process understanding (Musvoto et al. 2000, Ekama et al. 2006) or equilibrium predictors (Antony et al. 2011) (Barat et al. 2011, Huber et al. 2012, Joss et al. 2011). In the present study, an additional approach was also applied using kinetic parameter confidence for various minerals in a kinetic model description. Via this statistical approach, the formation of a mineral was deemed to be significant, if the kinetic parameter for that mineral was found to be significant (that is, the lower bound of the 95% confidence interval of the parameter should not be zero or negative). This approach is recognised as another approach which could be used alongside prior knowledge and equilibrium predictors.

## 3. Results

297 *3.1 Precipitating minerals*

298

299 Table 2 gives the measured compositions of the 3 wastewater samples (*synthetic wastewater*,
300 *sludge digestate* and *piggery digestate*). The *synthetic wastewater* contained magnesium
301 (Mg), calcium (Ca), phosphate ($PO_4$) and inorganic nitrogen (the relevant form being
302 ammonium, $NH_4$+) which could precipitate as struvite ($MgNH_4PO_4.6H_2O$) (Doyle et al.
303 2000), dicalcium phosphate dihydrate (DCPD, $CaHPO4.2H_2O$), amorphous calcium
304 phosphate (ACP, $Ca_3PO_4$) and octacalcium phosphate (OCP, $Ca_4H(PO4)_3.2.5H_2O$) (van
305 Kemenade and de Bruyn 1987). The *sludge digestate* and *piggery digestate* also contained a
306 considerable amount of Ca, Mg, $NH_4$+ and carbonate ($CO_3^{-2}$), but $PO_4$ was low in *piggery*
307 *digestate* and had to be added to provide realistic conditions for precipitation. According to
308 the relevant literature, the *sludge digestate* and the phosphate-spiked *piggery digestate* could
309 support the precipitation of struvite, magnesium phosphate (Abbona et al. 1982), calcium
310 carbonate ($CaCO_3$) (Nancollas and Reddy 1971) and calcium phosphate (van Kemenade and
311 de Bruyn 1987).

312

313 *3.1.1. Experiment 1: synthetic wastewater with titration*

314 An increase in pH (Fig. 1A) led to formation of precipitates, with a corresponding decrease in
315 soluble phosphate (Fig. 1B) and calcium (Fig. 1E). This is related to formation of a calcium
316 phosphate mineral (the model suggested DCPD), which became supersaturated and
317 precipitated around 1.8 h. As the pH continued to increase with time (for around 3.5 hours),
318 further decreases in calcium, magnesium, inorganic nitrogen and phosphate was observed,
319 suggesting that other minerals became supersaturated and precipitated, such as struvite and
320 OCP (see Figs. 1B, 1C, 1D and 1E). When two or more precipitates formed, competition
321 between the minerals was well described inherently by the model. In this case, key

competitive minerals appeared to include struvite and calcium phosphate (model indicated DCPD and OCP). The competition between these multiple minerals caused the complex interactions between pH, phosphates, and relevant cations observed in Figs. 1B, 1C, 1D and 1E. Fig. 2 presents a summary of parameter confidence regions for *Experiment 1*. An analysis of Fig. 2 shows that the parameter space of the 95% confidence regions for the three parameters ($k_{Struv}$ on the x-axis, $k_{DCPD}$, on the y-axis and $k_{OCP}$ on the z-axis) was generally right-asymmetric, particularly for the fast forming minerals (e.g. Struvite).

*3.1.2 Experiment 2: piggery digestate with aeration*

Fig. 3 presents experimental data and model results for the aeration test with *piggery digestate* (*Experiment 2*). In this experiment, the pH was increased by $CO_2$ stripping via continuous aeration, leading to a decrease in soluble inorganic carbon. Soluble magnesium, phosphate and inorganic nitrogen also immediately started to decrease when air flow was started. However, the decrease in soluble calcium was delayed by about 10 hours. This specifically is described by relatively rapid struvite formation ($k_{Struv}$ =12±10 $h^{-1}$, Table 3) and relatively slow calcium carbonate monohydrate (CCM) formation ($k_{CCM}$=0.36±0.03 $h^{-1}$, Table 3). Fig. 3G illustrates the joint confidence region of the parameters in *Experiment 2*. As shown in the upper-unlimited/unbounded confidence region, any arbitrarily high $k_{cryst}$ value would have been suitable for struvite (x-axis), while calcium carbonate kinetic coefficient values were tightly bound (y-axis).

*3.1.3. Experiment 3: sludge digestate with aeration*

Fig. 4 presents simulation and experimental results for the aeration experiment with *sludge digestate* (*Experiment 3*). In this experiment, pH increased due to $CO_2$ stripping by aeration. Measured calcium, magnesium, phosphate and inorganic nitrogen decreased over time (Figs.

4C-F), probably by the precipitation of struvite and calcium phosphate minerals (model indicated ACP). The competition with time among minerals was driven by the dynamic of pH change and availability of calcium, magnesium, phosphate, total inorganic carbon and inorganic nitrogen. However, in this *Experiment 3*, ACP ($k_{ACP}$ = 3.2±1 $h^{-1}$, Table 3) was observed to have similar kinetic rates to struvite ($k_{Struv}$ =4.5±1.3 $h^{-1}$, Table 3), indicating that these two minerals were strongly competing. Formation of calcium carbonate (CCM) was very limited in *Experiment 3*, such that the $k_{CCM}$ value was not significantly different from zero (0 - 0.2 $h^{-1}$). In such a case, CCM could either be eliminated, or retained in the model with an arbitrarily low kinetic coefficient, depending on its importance as an output. Fig. 4G shows kinetic parameter confidence regions for struvite and ACP in *Experiment* 3. Unlike *Experiment 2*, the confidence region here was bounded symmetric, indicating that the model was slightly more tolerant to higher values of kinetic coefficients for these strongly competing minerals, but in general, parameter correlation was low, indicating that parameter values for individual minerals could be independently fitted (keeping all other model parameters constant).

*3.3 Model prediction capability*

To test the model prediction capability, the fitted parameters from one set of experiments (Experiments 1-3, parameters in Table 3) were reused to predict dynamics for repeat experiments, under slightly different conditions. The results, which are presented in the supplementary material (Figures S1, S2 and S3), showed that parameters would probably be transferable within wastewaters, with slightly different operating conditions. Prediction of pH and dynamic state variables was very good and consistent. The only instance of poor

prediction was over-prediction of TIC in one experiment (See Figure S3), probably due to differences in $CO_2$ exchange and thus $k_La$.

*3.2 Influence of TSS on precipitation kinetics*

Further model analysis tested the influence of wastewater total suspended solids on the precipitation kinetic rate, and sought to justify the use of $X_{\mathrm{cryst}}$ for multiple minerals precipitation. For this purpose, Experiment 4 trialled three different native TSS concentrations. The dataset for Experiment 4 was adequately fitted with a single set of parameter values, which were (given with linear estimates of confidence) $k_{\mathrm{Struvt}}$ = 33.1±13.1 $h^{-1}$ and $k_{\mathrm{DCPD}}$ = 53.1±13.7 $h^{-1}$ for struvite and DCPD, respectively. Fig. 5 presents the fit together with the experimental data and shows that the baseline model fit all three experiments qualitatively well. The final concentrations of Mg, PO4-P and NH4-N in all the three experiment were within the same range, indicating that struvite formation was insensitive to TSS. However, calcium did show a discrepancy between the lowest TSS and the higher two TSS conditions, indicating a variable influence of TSS on calcium minerals precipitation.

## 4 Discussion

*4.1 Significance of parameter ranges*

Based on the results above, minerals can be classed as either rapidly forming ($k_{\mathrm{cryst}}$>5 $h^{-1}$ – struvite, ACP), moderately forming ($k_{\mathrm{cryst}}$~>1 $h^{-1}$ – DCPD, OCP) or slow forming ($k_{\mathrm{cryst}}$<0.5 $h^{-1}$ – calcium carbonate in real wastewater). In at least one case (*Experiment 3*), calcium

carbonate mineral formation was substantially retarded (<0.2 $h^{-1}$), but in general, minerals precipitation rates were consistent across all three experiments. This indicated that kinetic rate parameters may be transferable across different systems. Parameters could be confidence-bounded or unbounded. Where parameters were unbounded, they were observed to be highly asymmetric and nonlinear (Fig. 3G), with model-data residuals generally increasing more gradually with larger coefficient values than the identified optimum. These findings indicated that the model was more tolerant to high values of kinetic rate coefficients (i.e. fast precipitation kinetics). This is in agreement with other studies (Musvoto et al. 2000, van Rensburg et al. 2003, Ekama et al. 2006, Kazadi Mbamba et al, 2015) that reported on dominance and fast precipitation kinetics in wastewater. Further, Kazadi Mbamba et al. (2015) suggested that when process data was lacking for machine parameter estimation, arbitrarily high values of precipitation kinetic rate coefficients could be selected to provide realistic estimates of precipitation rates. However, based on the present results (*Experiments 2 and 3*), wastewater conditions could retard or slow the formation of some minerals, such as calcium carbonate monohydrate, for which arbitrarily high kinetic rate coefficients may then not be suitable. This offers the possibility to class minerals as fast, or slow forming, with fast forming minerals being given arbitrarily high kinetic parameters (e.g. $k_{cryst}$=5 $h^{-1}$), and slow forming minerals being given order of magnitude low kinetic parameter values (e.g. $k_{cryst}$=0.1 $h^{-1}$). Alternatively, depending on the system retention times, a slow forming mineral may be completely excluded from a model (particularly where the parameter confidence interval overlaps the zero vector). The kinetic value of fast minerals may only become important under specific cases (e.g., with small reactors for dedicated struvite crystallisation). Finally, it is important to note that even where minerals shared solutes (DCPD, OCP), parameter correlation was low (*Experiment* 1). Accordingly, where multiple minerals are forming, it could be possible to independently consider individual minerals in the model fit.

The estimated parameters obtained in the present study were lower than values reported by other studies (Musvoto et al. 2000, van Rensburg et al. 2003). This difference could be explained to some extent by differences in model structure and the composition of wastewaters used. For instance, Musvoto et al. (2000) suggested that kinetic rate coefficients may not be transferable between different wastewaters and could vary by several orders of magnitude for wastewaters of markedly different composition. They ascribed these discrepancies to the presence of dissolved organic matter and inorganic constituents which could act as inhibitors. In general, a parameter estimation routine could provide confidence in kinetic parameters in cases where sufficient process data is available for such analyses to be performed.

*4.2 Model performance*

The proposed model was able to reproduce the dynamics of state variables and provided an indication of relevant minerals. There were some minor dynamics that were not accounted for by the model (e.g., around 1.8 hrs in *Experiment 1*), which could have been caused by secondary mechanisms such as sorption of magnesium ions onto/into calcium phosphate precipitates (Ferguson and McCarty 1971). This is seen in Fig. 1C where the concentration of soluble magnesium decreased with calcium and phosphate before a substantial decrease in inorganic nitrogen was observed around 3.5 h (Fig. 1D). A sorption process is likely unnecessarily complex for most conventional wastewater treatment models and is most likely to cause discrepancies during highly transient conditions (particularly batch) (Kazadi Mbamba et al, 2015). The formation of other minerals such as dolomite was also explored, but their inclusion did not significantly improve model performance.

The proposed kinetic rate expression with $X_{cryst}$ and dependency on supersaturation provides a compact semi-mechanistic description suitable for coupling with biological models, and places a limit on precipitation rates to handle nucleation induction kinetics. Further, the combined equilibrium description based on thermodynamics provides a reliable estimate of saturation extents and does not introduce additional fitted parameters. Other studies (Musvoto et al., 2000) have applied a kinetic approach for both fast reactions (acid-base systems) and slow reactions, which works well, but increases the number of dynamic state variables and can introduce model stiffness (Rosen et al., 2005). A recent study by Lizarralde et al. (2015) models precipitation kinetics based on constant specific surface area and Monod-style kinetics in mineral state, instead of the linear dependency on $X_{cryst}$ used in the present study. The rate expression of Lizarralde et al. handles nucleation induction kinetics by an additional monod-style term in supersaturation, rather than the approach of the present study using small initial values of $X_{cryst}$ for nucleation induction kinetics (Kazadi Mbamba et al. 2015). Both approaches may be valid but require considerable future work with experimental validation. However, in regards to the use of TSS as a lumped reference state for kinetics, the findings from the present study (particularly for Experiment 4) suggested that native TSS does not necessarily dictate kinetics. In particular, struvite kinetics in Experiment 4 was largely insensitive to TSS content, whereas calcium precipitation was influenced to varied extents. Thus, it is suggested that the use of $X_{cryst}$ is preferred as a reference state instead of TSS. Albeit, that in a continuous digester or wastewater process, the net effect may be the same, because the recycled pool of seed lies as a fraction within TSS.

*4.3 Model applications*

Multiple mineral precipitation modelling is important to reliably describe major chemical states in standard models (e.g. ASM series; Henze et al. 2000; ADM 1; Batstone et al. 2012) in a plant-wide platform (e.g. Benchmark Simulation Model (BSM2); Gernaey et al., 2014). Particularly, with the recycling of minerals in sludge, phosphorus, sulphur and major metals are exchanged between wastewater and minerals. Findings from the present study showed that only a few minerals may need to feature in realistic plant-wide descriptions, although such may be site or system-specific (Henze et al. 2000). With retention of mineral phases in sludge lines, a parallel precipitation modelling approach with dependency on mineral state ($X_{cryst}$) is useful (as used in the present study), because mineral states can be approximately tracked to capture longer-term effects in the plant-wide modelling context. For example, struvite started to precipitate immediately in *Experiments 2* and *3*, which showed that the existing struvite available in the wastewater was sufficient to drive and support precipitation (no nucleation induction was observed). In addition, Kazadi Mbamba et al (2015) noted that the approach of including a small arbitrary amount of mineral phase in the initial conditions of the model, was capable of continuously capturing minerals precipitation driven by either pre-existing mineral phase (such as struvite in the present study) and/or minerals precipitation dictated by nucleation induction kinetics. Minerals precipitation modelling is also important in emerging applications such as nutrient and resource recovery. In such cases, a combined kinetic-equilibrium precipitation model (Section 2.5) with machine estimation of kinetic parameters, can support system design as well as provide a measure of equilibrium yield.

## 5. Conclusions

A precipitation modelling approach proposed by Kazadi Mbamba et al. (2015) was validated with multiple minerals, via dynamic titration experiments with precipitation in synthetic

wastewater, and via aerated precipitation experiments in real wastewaters. The results showed that the model was identifiable and performed well at quantitatively describing the (parallel) precipitation of struvite, and calcium carbonate and calcium phosphate minerals. Minerals could be broadly classed on the basis of kinetic rate coefficient as either rapidly forming/strongly competing ($k_{cryst}$>5 $h^{-1}$), moderately forming ($k_{cryst}$ >1 $h^{-1}$), and slow forming ($k_{cryst}$ <0.5 $h^{-1}$). Since the precipitation model equation set is kinetic-based, it can be readily integrated with biological reactions (e.g. ASM2d and ADM1) in plant-wide models used across the wastewater sector.

## Acknowledgment

This research was supported financially by the University of Queensland through the UQ International Scholarships (UQI) and the UQ Collaboration and Industry Engagement Fund (UQCIEF). Dr Flores-Alsina fully acknowledges the financial support of the EU 7th Framework Programme FP7/2007-2013 under the REA agreement 329349 (PROTEUS). Dr. Beatrice Keller-Lehmann (AWMC, UQ) and Mr. Nathan Clayton (AWMC) performed chemical analyses of wastewater samples.

## Software availability

The implementation of the weak acid-base chemistry plus the multiple precipitation model will be distributed for free upon request to Dr Damien Batstone (damienb@awmc.up.edu.au) at University of Queensland (Australia).

519 # References

520

521 Abbona, F., Lundager Madsen, H.E. and Boistelle, R., 1982. Crystallization of two
522 magnesium phosphates, struvite and newberyite: Effect of pH and concentration. Journal of
523 Crystal Growth 57(1), 6-14.

524 Antony, A., Low, J.H., Gray, S., Childress, A.E., Le-Clech, P. and Leslie, G., 2011. Scale
525 formation and control in high pressure membrane water treatment systems: A review. Journal
526 of Membrane Science 383(1–2), 1-16.

527 Barat, R., Montoya, T., Seco, A. and Ferrer, J., 2011. Modelling biological and chemically
528 induced precipitation of calcium phosphate in enhanced biological phosphorus removal
529 systems. Water Research 45(12), 3744-3752.

530 Batstone, D.J., 2006. Mathematical modelling of anaerobic reactors treating domestic
531 wastewater: Rational criteria for model use. Reviews in Environmental Science and
532 Bio/Technology 5(1), 57-71.

533 Batstone, D.J. and Keller, J., 2003. Industrial application of the IWA anaerobic digestion
534 model No. 1 (ADM). Water Science and Technology 47(12, 199-206.

535 Batstone, D.J., Amerlinck, Y., Ekama, G.A., Goel, R., Grau, P., Johnson, B., Kaya, I., Steyer,
536 J.-P., Tait, S., Takács, I., Vanrolleghem, P.A., Brouchaert, C.J. and Volcke, E., 2012.
537 Towards a generalised physicochemical modelling framework. Water Science and
538 Technology 66(6), 1147-1161.

539 Batstone, D.J., Keller, J. and Steyer, J., 2006. A review of ADM 1 extensions, applications,
540 and analysis: 2002-2005. Water Science and Technology 54(4), 1-10.

541 Batstone, D.J., Keller, J., Kalyuzhnyi, S.V., Pavlostathis, S.G., Rozzi, A., Sanders, W.T.M.,
542 Siegrist, H. and Vavilin, V.A., 2002. Anaerobic digestion model no. 1, IWA Publishing,
543 London.

544 Batstone, D.J., Pind, P.F. and Angelidaki, I., 2003. Kinetics of thermophilic, anaerobic
545 oxidation of straight and branched chain butyrate and valerate. Biotechnology and
546 Bioengineering 84(2), 195-204.

547 Brečević, L. and Nielsen, A.E., 1989. Solubility of amorphous calcium carbonate. Journal of
548 Crystal Growth 98(3), 504-510.

549 Chen, Y., Cheng, J.J. and Creamer, K.S., 2008. Inhibition of anaerobic digestion process: A
550 review. Bioresource Technology 99(10), 4044-4064.

551 Doyle, J.D. and Parsons, S.A., 2002. Struvite formation, control and recovery. Water
552 Research 36(16), 3925-3940.

553 Doyle, J.D., Philp, R., Churchley, J. and Parsons, S.A., 2000. Analysis of Struvite
554 Precipitation in Real and Synthetic Liquors. Process Safety and Environmental Protection
555 78(6), 480-488.

556 Ekama, G.A., Wentzel, M.C. and Loewenthal, R.E., 2006. Integrated chemical-physical
557 processes kinetic modelling of multiple mineral precipitation problems. Water Science and
558 Technology 53(12), 65-73.

559 Ferguson, J.F. and McCarty, P.L., 1971. Effects of carbonate and magnesium on calcium
560 phosphate precipitation. Environmental Science & Technology 5(6), 534-540.

561 Gernaey, K.V., Jeppsson, U., Vanrolleghem, P.A. and Copp, J.B., 2014. Benchmarking of
562 control strategies for wastewater treatment plants, IWA Publishing.

563 Henze, M., Gujer, W., Mino, T. and van Loosdrecht, M., 2000. Activated sludge models
564 ASM1, ASM2, ASM2d and ASM3, IWA Publishing, London.

565 Huber, P., Nivelon, S., Ottenio, P. and Nortier, P., 2012. Coupling a Chemical Reaction
566 Engine with a Mass Flow Balance Process Simulation for Scaling Management in
567 Papermaking Process Waters. Industrial & Engineering Chemistry Research 52(1), 421-429.

568 Joss, A., Baenninger, C., Foa, P., Koepke, S., Krauss, M., McArdell, C.S., Rottermann, K.,
569 Wei, Y., Zapata, A. and Siegrist, H., 2011. Water reuse: >90% water yield in MBR/RO
570 through concentrate recycling and CO2 addition as scaling control. Water Research 45(18),
571 6141-6151.

572 Kazadi Mbamba, C., Batstone, D.J., Flores-Alsina, X. and Tait, S., 2015. A generalised
573 chemical precipitation modelling approach in wastewater treatment applied to calcite. Water
574 Research 68(0), 342-353.

575 Kralj, D., Brečević, L. and Kontrec, J., 1997. Vaterite growth and dissolution in aqueous
576 solution III. Kinetics of transformation. Journal of Crystal Growth 177(3–4), 248-257.

577 Le Corre, K.S., Valsami-Jones, E., Hobbs, P. and Parsons, S.A., 2009. Phosphorus Recovery
578 from Wastewater by Struvite Crystallization: A Review. Critical Reviews in Environmental
579 Science and Technology 39(6), 433-477.

580 Lizarralde, I., Fernández-Arévalo, T., Brouckaert, C., Vanrolleghem, P., Ikumi, D. S., Ekama,
581 G. A., Grau, P. (2015). A new general methodology for incorporating physico-chemical
582 transformations into multi-phase wastewater treatment process models. Water research, 74,
583 239-256.

584 Lobry, J., Rosso, L. and Flandrois, J., 1991. A FORTRAN subroutine for the determination of
585 parameter confidence limits in non-linear models. Binary 3, 86-93.

586 Mehta, C.M. and Batstone, D.J., 2013. Nucleation and growth kinetics of struvite
587 crystallization. Water Research 47(8), 2890-2900.

588 Meyer, J.L. and Weatherall, C.C., 1982. Amorphous to crystalline calcium phosphate phase
589 transformation at elevated pH. Journal of Colloid And Interface Science 89(1), 257-267.

590 Morel, F.M.M. and Hering, J.G., 1993. Principles and applications of aquatic chemistry,
591 Wiley, New York.

592 Mullin, J.W., 2001. Crystallization, Elsevier Butterworth-Heinemann, Oxford.

593 Musvoto, E.V., Wentzel, M.C. and Ekama, G.A., 2000. Integrated chemical–physical
594 processes modelling—II. simulating aeration treatment of anaerobic digester supernatants.
595 Water Research 34(6), 1868-1880.

596 Nancollas, G.H. and Reddy, M.M., 1971. The crystallization of calcium carbonate. II. Calcite
597 growth mechanism. Journal of Colloid And Interface Science 37(4), 824-830.

598 Nielsen, A.E., 1984. Electrolyte crystal growth mechanisms. Journal of Crystal Growth 67(2),
599 289-310.

600 Ohlinger, K.N., Young, T.M. and Schroeder, E.D., 1998. Predicting struvite formation in
601 digestion. Water Research 32(12), 3607-3614.

Rosen, C., Vrecko, D., Gernaey, K. V., and Jeppsson, U., 2005. Implementing ADM1 for benchmark simulations in Matlab/Simulink. Paper presented at the Proceedings of the First International Workshop on the IWA anaerobic Digestion No. 1 (ADM1), Lyngby, Denmark.

Skerman, A. and Collman, G., 2012. Methane Recovery and use at Grantham Piggery, RIRDC Publication No. 12/064, RIRDC Project No. PRJ-005672. Available at https://rirdc.infoservices.com.au/items/12-064).

Solon, K., Flores-Alsina, X., Kazadi Mbamba, C., Volcke, E.I.P., Tait, S., Batstone, D., Gernaey, K.V. and Jeppsson, U., 2015. Effects of ionic strength and ion pairing on (plant-wide) modelling of anaerobic digestion. Water Research 70(0), 235-245.

Stumm, W. and Morgan, J.J., 1996. Aquatic chemistry: chemical equilibria and rates in natural waters, Wiley, New York.

van Kemenade, M.J.J.M. and de Bruyn, P.L., 1987. A kinetic study of precipitation from supersaturated calcium phosphate solutions. Journal of Colloid And Interface Science 118(2), 564-585.

van Langerak, E.P.A., Ramaekers, H., Wiechers, J., Veeken, A.H.M., Hamelers, H.V.M. and Lettinga, G., 2000. Impact of location of CaCO3 precipitation on the development of intact anaerobic sludge. Water Research 34(2), 437-446.

van Rensburg, P., Musvoto, E.V., Wentzel, M.C. and Ekama, G.A., 2003. Modelling multiple mineral precipitation in anaerobic digester liquor. Water Research 37(13), 3087-3097.

Flores-Alsina, X., Kazadi Mbamba, C., Solon, K., Darko Vrecko, D., Tait, S., Batstone, D., Jeppsson, U., Gernaey, K., 2015. A plant-wide aqueous phase chemistry module describing pH variations and ion speciation/pairing in wastewater treatment process models. Water Research (Accepted).

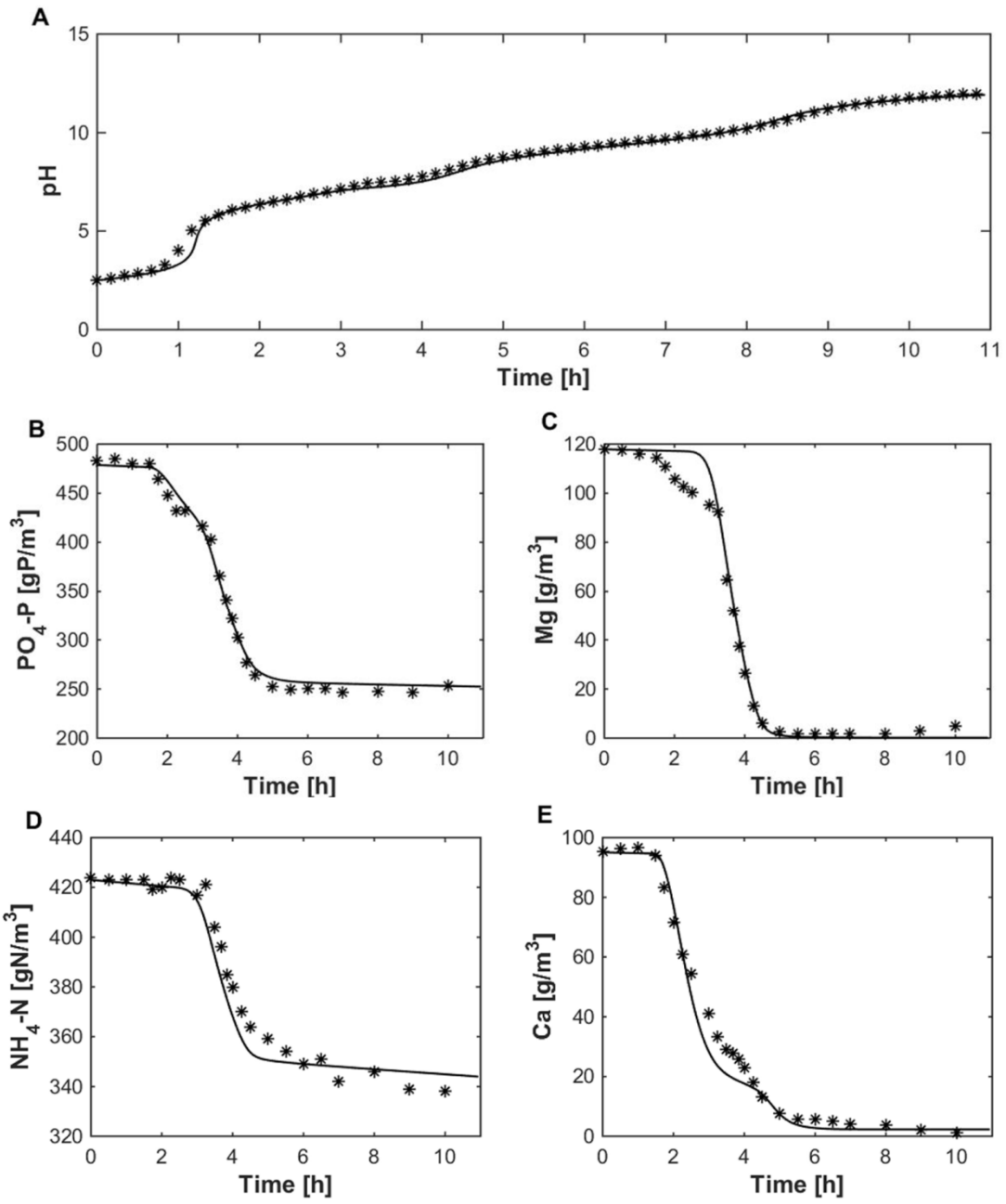


633

634 **Fig. 1 – Experimental data and model fits for *Experiment 1* with titration tests on**
635 ***synthetic wastewater*, expected to precipitate out struvite, dicalcium phosphate dihydrate**
636 **(DCPD), amorphous calcium phosphate (ACP) and octacalcium phosphate (OCP). The**
637 **lines show simulation results using the optimum parameter values listed in Table 3.**

638

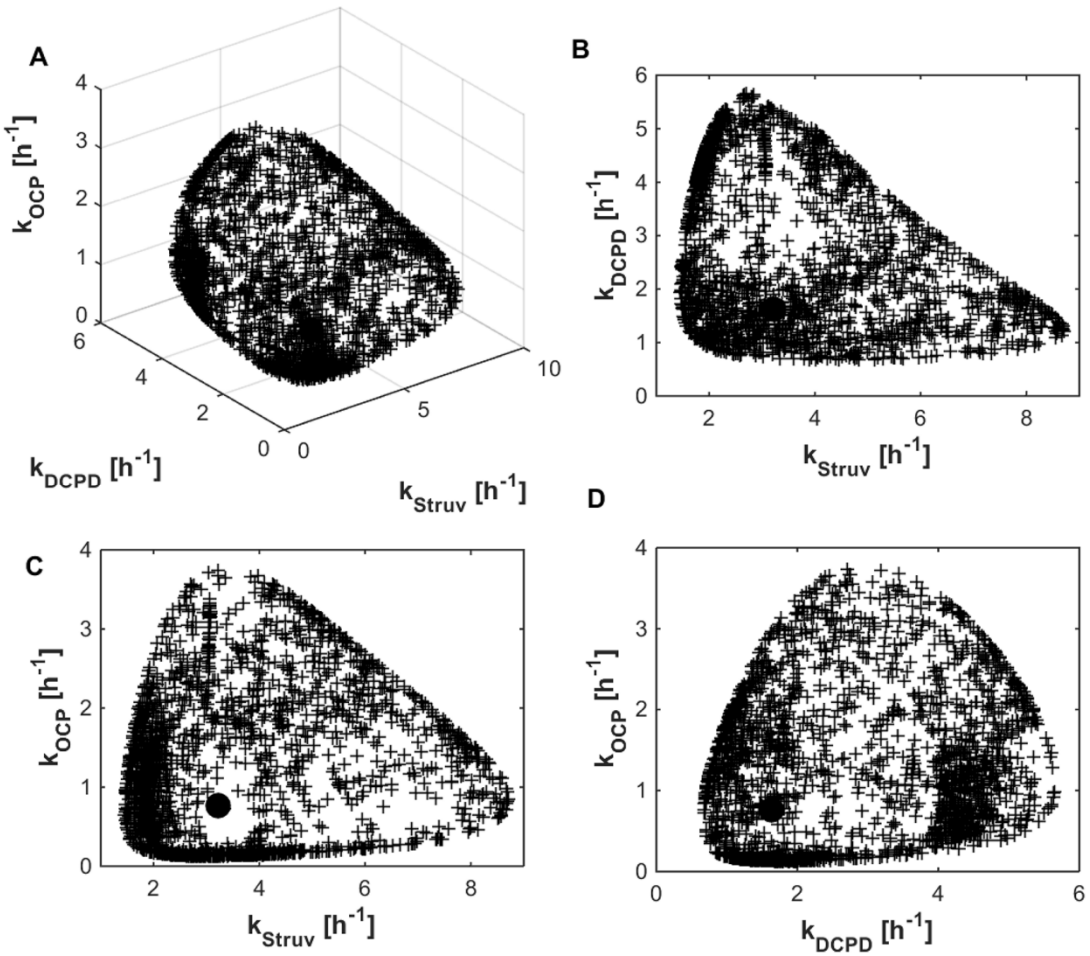


639

640 **Fig. 2 – Confidence regions at the 95% confidence limit for kinetic parameters**
641 **determined from model fits of data from *Experiment 1* – Titration with *synthetic***
642 ***wastewater*. The confidence region is presented as a three-dimensional volume (A) and as**
643 **two-dimensional projections on three different X-Y planes (B, C, D), with fitted kinetics**
644 **for the minerals struvite (Struv), octacalcium phosphate (OCP) and dicalcium**
645 **phosphate dihydrate (DCPD). The large dots are the optimum values listed in Table 3.**

646

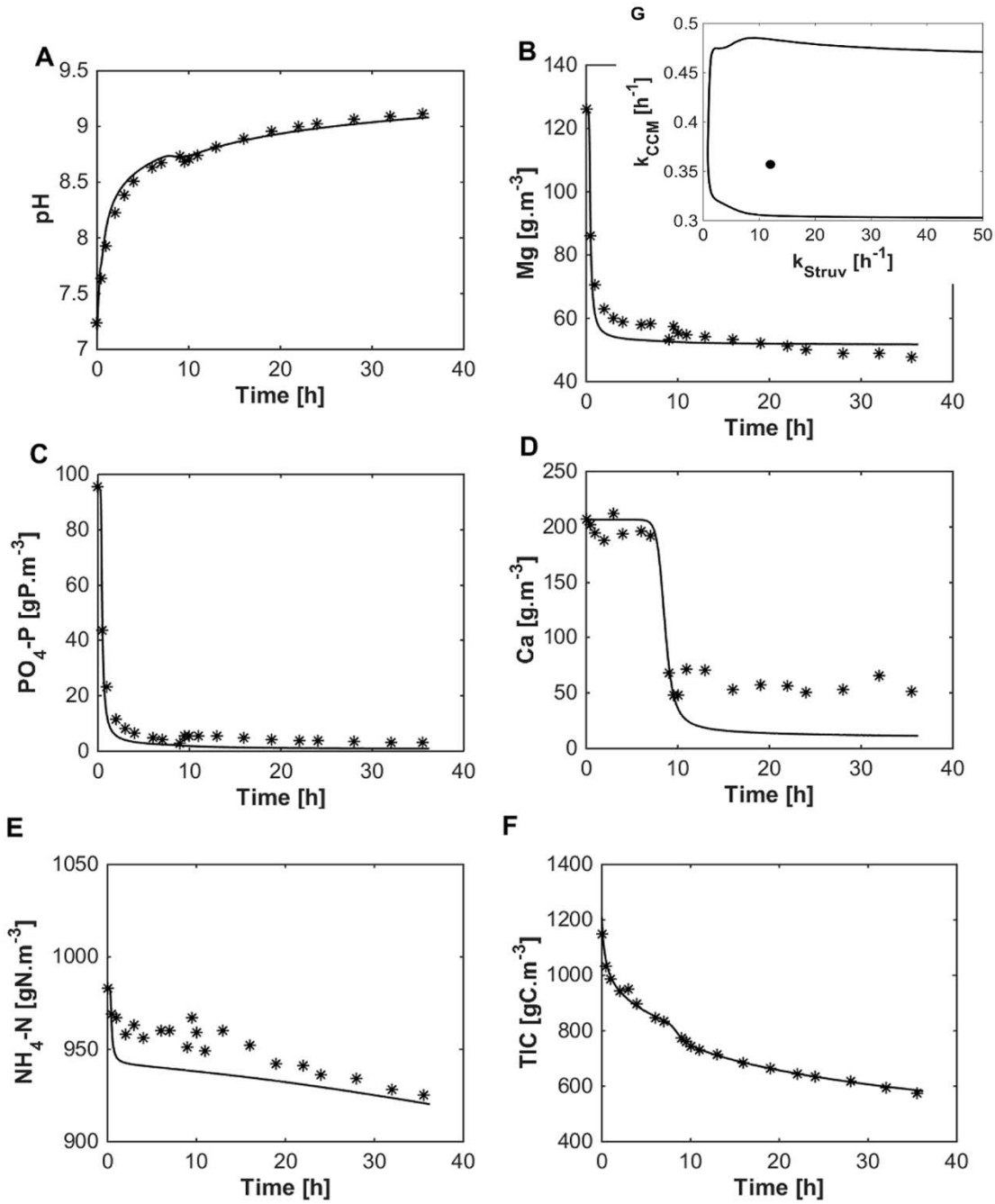


**Fig. 3 – Experimental data and modelling fits for *Experiment 2* with aeration tests on *piggery digestate*. The lines show the simulaton results using the optimum kinetic parameter values listed in Table 3. An in-lay (G) presents confidence regions at the 95% confidence limit for fitted kinetic parameters of the minerals struvite (Struv) and calcium carbonate (monohydrate) (CCM).**

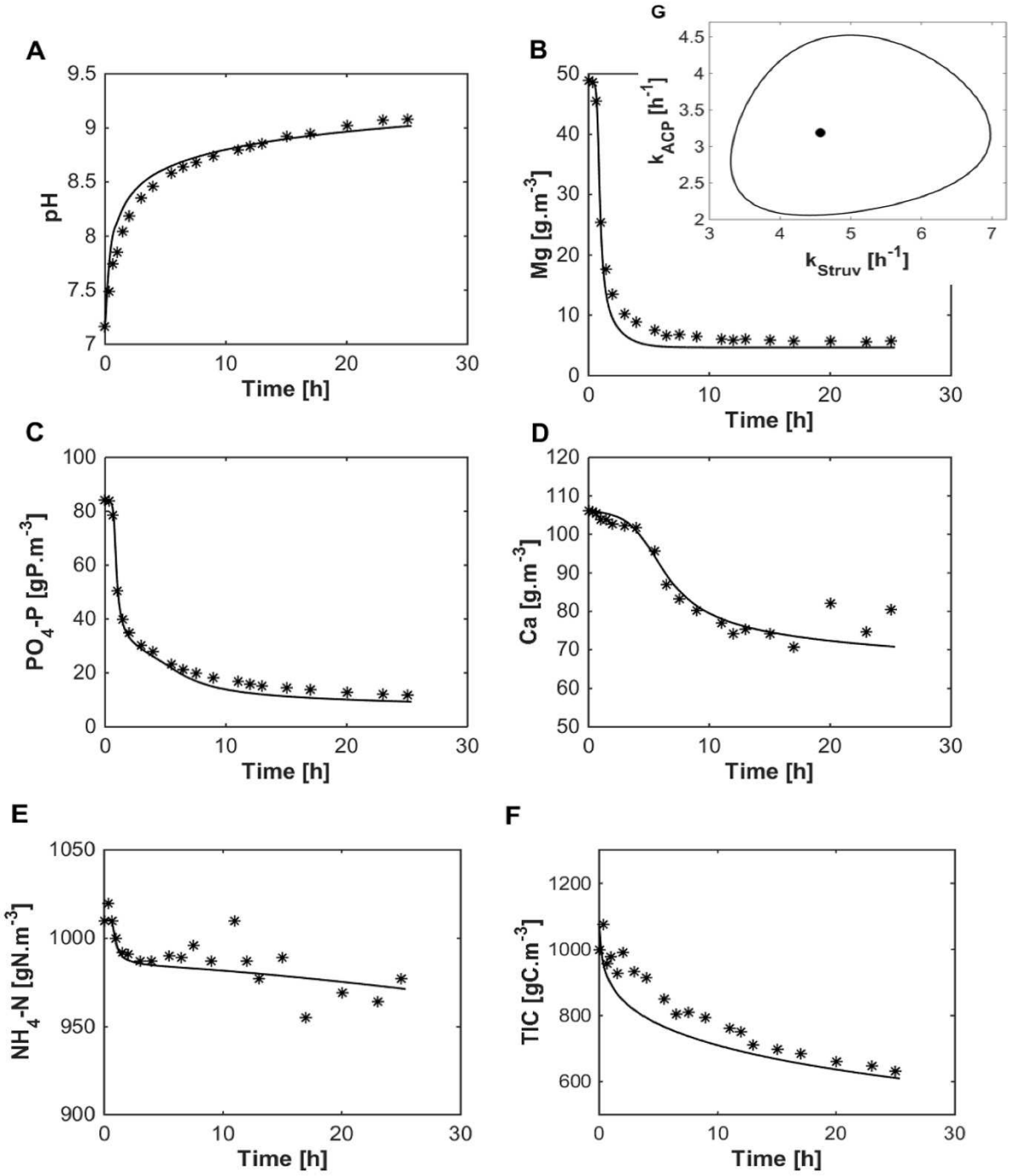


655

656 **Fig. 4 – Representative experimental and modelling data for the precipitation**
657 ***Experiment 3* - aeration tests with *sludge digestate*. The symbols and the solid lines**
658 **represent the experimental and simulation results, respectively. The simulation used the**
659 **optimum parameter values listed in Table 3. An in-lay (G) presents confidence regions**

660 **at the 95% confidence limit for fitted kinetic parameters of the minerals struvite (Struv)**

661 **and amorphous calcium phosphate (ACP).**

662

663

664

665

666

667

668

669

670

671

672

673

674

675

676

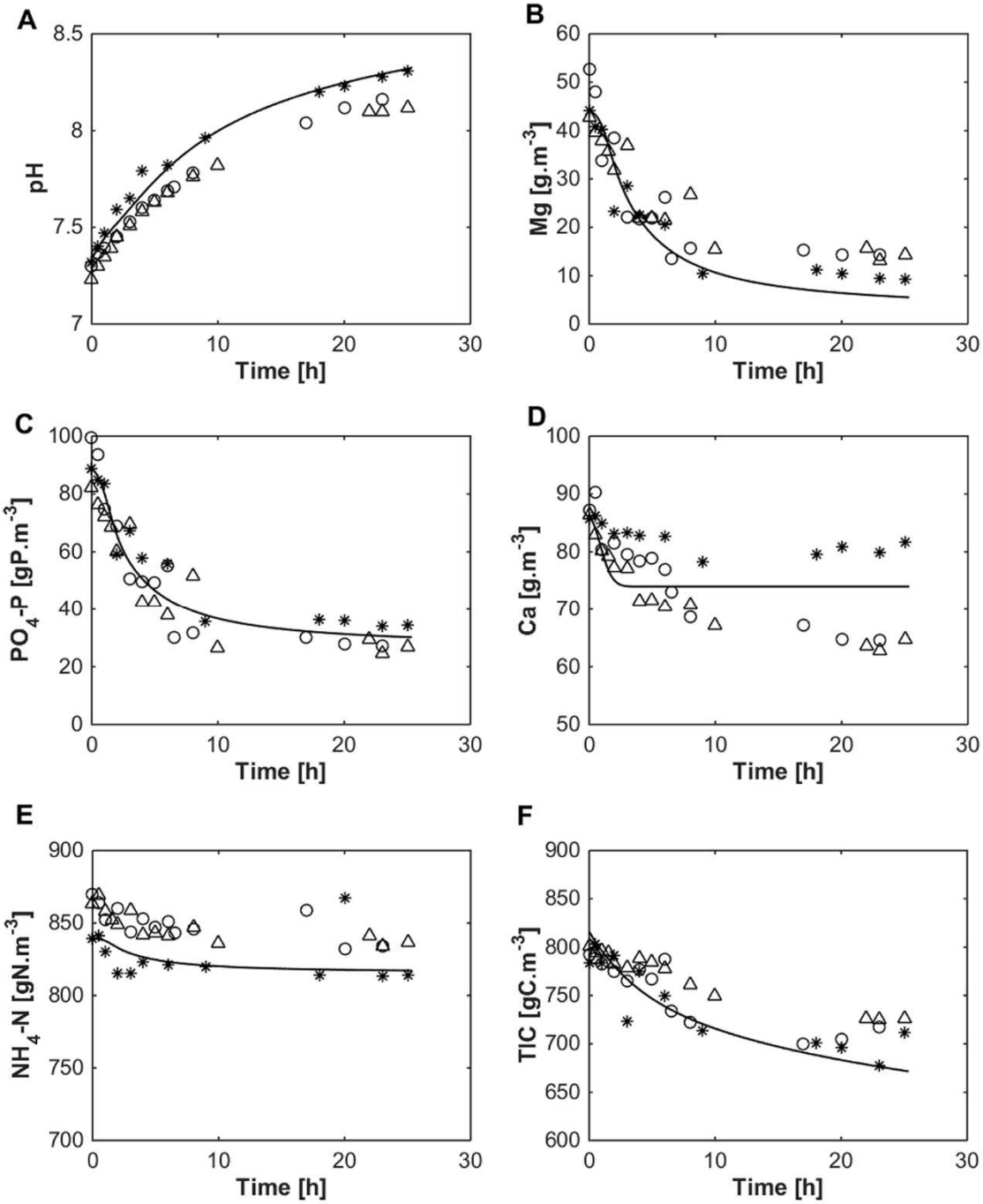


677

678

679 **Fig. 5 - Data from three aeration tests with *sludge digestate* under three different initial**

680 **TSS concentrations 1118 gTSS.m$^{-3}$ (*), 4002 gTSS.m$^{-3}$ (o), 10959 gTSS.m$^{-3}$ (Δ) gave**

681 **$k_{Struvite}$ = 33.1±13.1 h$^{-1}$ and $k_{DCPD}$ = 53.1±13.7 h$^{-1}$.**

682

683

684

**Table 1 Stoichiometric matrix format showing kinetic rate equations and equilibrium constants for the precipitation/dissolution processes**

| Precipitation processes | Stoichiometry | | | | | | Rate equations | Equilibrium constants |
|---|---|---|---|---|---|---|---|---|
| | $H^+$ | $NH_4^+$ | $Ca^{2+}$ | $Mg^{2+}$ | $CO_3^{2-}$ | $PO_4^{3-}$ | | |
| Amorphous calcium phosphate (ACP) | | | +/-3 | | | +/-2 | $k_{ACP} \times X_{ACP}\left[\left(\frac{\left(S_{(Ca^{2+})}\right)^3 \times \left(S_{(PO_4^{3-})}\right)^2}{K_{\mathrm{spACP}}}\right)^{1/5} - 1\right]^2$ | $pK_{sp,ACP}$=25.46 [a] |
| Calcium carbonate monohydrate (CCM) | | | +/-1 | | +/-1 | | $k_{\mathrm{CCM}} \times X_{\mathrm{CCM}}\left[\left(\frac{S_{(Ca^{2+})} \times S_{(CO_3^{2-})}}{K_{spDCPD}}\right)^{1/2} - 1\right]^2$ | $pK_{sp,CCM}$=7.144 [a] |
| Dicalcium phosphate hydrate (DCPD) | +/-1 | | +/-1 | | | +/-1 | $k_{\mathrm{DCPD}} \times X_{\mathrm{DCPD}}\left[\left(\frac{S_{(Ca^{2+})} \times S_{(H^+)} \times S_{(PO_4^{3-})}}{K_{spDCPD}}\right)^{1/3} - 1\right]^2$ | $pK_{sp,DCPD}$=18.99 [a] |
| Octacalcium phosphate (OCP) | +/-1 | | +/-4 | | | +/-3 | $k_{OCP} \times X_{OCP}\left[\left(\frac{S_{(H^+)} \times \left(S_{(Ca^{2+})}\right)^4 \times \left(S_{(PO_4^{3-})}\right)^3}{K_{\mathrm{spOCP}}}\right)^{1/8} - 1\right]^2$ | $pK_{sp,OCP}$=47.95 [a] |
| Struvite | | +/-1 | | +/-1 | | +/-1 | $k_{Struv} \times X_{Struv}\left[\left(\frac{S_{(Mg^{2+})} \times S_{(NH_4^+)} \times S_{(PO_4^{3-})}}{K_{spStruv}}\right)^{1/3} - 1\right]^3$ | $pK_{sp,Struv}$=13.26 [b] |

$k_{\mathrm{Struv}}$, $k_{\mathrm{DCPD}}$, $k_{\mathrm{ACP}}$, $k_{\mathrm{CCM}}$ and $k_{\mathrm{OCP}}$ are the empirical kinetic rate coefficients ($min^{-1}$) for Struvite, DCPD, ACP, CCM and OCP, respectively. $X_{\mathrm{Struv}}$, $X_{\mathrm{DCPD}}$, $X_{\mathrm{ACP}}$, $X_{\mathrm{CCM}}$ and $X_{\mathrm{OCP}}$ are the concentrations (moles/L) of Struvite, DCPD, ACP, CCM and OCP, respectively. $K_{\mathrm{spStruv}}$, $K_{\mathrm{spDCPD}}$, $K_{\mathrm{spACP}}$, $K_{\mathrm{spCCM}}$, and $K_{\mathrm{spOCP}}$ are the solubility constants for Struvite, DCPD, ACP and OCP, respectively. $S_{(Mg+2)}$, $S_{(NH4+)}$, $S_{(PO4-3)}$, $S_{(Ca+2)}$, $S_{(CO3-2)}$ and $S_{(H+)}$ are the chemical activities of magnesium, ammonium, phosphate, calcium, carbonate and hydrogen ions, respectively, in the aqueous phase.

[a] Visual MINTEQ (Version 3.0, Royal Institute of Technology (KTH))

[b] (Ohlinger et al. 1998)

**Table 2 – Wastewater matrix characteristics**

| **Parameter** | Synthetic wastewater | Piggery digestate [a] | Sludge digestate [b] | Sludge digestate[c] | | |
|---|---|---|---|---|---|---|
| | | | | TS1 | TS2 | TS3 |
| Ammonia ( gNH4-N.m$^{-3)}$ | 423 | 983 | 1010 | 839 | 870 | 863 |
| Calcium ( g.m$^{-3}$) | 95 | 207 | 107 | 86 | 87 | 86 |
| Chloride ( g.m$^{-3}$) | 1815 | 1797 | 742 | | | |
| Iron ( g.m$^{-3}$) | 0 | 0.64 | 1.1 | | | |
| Magnesium ( g.m$^{-3}$) | 120 | 126 | 49 | 44 | 53 | 43 |
| Phosphorus ( gPO4-P.m$^{-3}$) | 479 | 96 | 84 | 89 | 99 | 82 |
| Potassium ( g.m$^{-3}$) | 0 | 989 | 164 | 126 | 129 | 129 |
| Sodium ( g.m$^{-3}$) | 336 | 712 | 481 | 400 | 411 | 410 |
| Sulphate ( g.m$^{-3}$) | 0 | 0.07 | 7.3 | | | |
| Sulphide ( g.m$^{-3}$) | 0 | 0.08 | 0.11 | | | |
| Total dissolved inorganic carbon (g.m$^{-3}$) | 0 | 1150 | 945 | 815 | 793 | 815 |
| Total suspended solid (gTSS.m$^{-3}$) | | | | 1118 | 4002 | 10959 |
| pH (standard) | 2.5 | 7.3 | 7.4 | 7.3 | 7.3 | 7.2 |

[a] Piggery digestate – the analysis was carried out on supernatant after addition of phosphate

[b] Sludge digestate – the analysis was carried out on the supernatant

[c] Sludge digestate – the analysis was carried out on three samples with different TSS concentrations

685

686

687

688

**Table 3 - Estimated optimum values for the kinetic coefficients in each of the three precipitation experiments, given with ± linear estimates of 95% confidence intervals estimated using two tailed t-student tests.**

| Kinetic coefficients | Experiments | | | |
|---|---|---|---|---|
| | 1–Titration in synthetic wastewater | 2 – Aeration in piggery digestate | 3 – Aeration in sludge digestate | 4 – Aeration in sludge digestate |
| $k_{Struv}$ | 3.2±1.0 | 12±10 | 4.49±1.3 | 33±13 |
| $k_{CCM}$ | | 0.36±0.03 | <0.2 | |
| $k_{ACP}$ | | | 3.15± 1 | |
| $k_{OCP}$ | 0.76±0.69 | | | |
| $k_{DCPD}$ | 1.63±0.49 | | | 53±14 |
| $k_La$ ($CO_2$) | | 5.5±0.5 | 5.5* | 0.35* |
| $k_La$ ($NH_3$) | | 0.003* | 0.003± 0.0013 | |

$k_{Struv}$, $k_{CCM}$, $k_{DCPD}$, $k_{ACP}$ and $k_{OCP}$ are the empirical kinetic rate coefficients ($h^{-1}$) for struvite, calcium carbonate monohydrate (CCM), dihydrate dicalcium phosphate (DCPD), amorphous calcium phosphate (ACP) and octacalcium phosphate (OCP), respectively.

$k_La$ ($CO_2$) and $k_La$ ($NH_3$) are the the overall film mass transfer coefficients ($h^{-1}$) for $CO_2$ and $NH_3$, respectively.

* Assumed value

# Highlights (for review)

- A systematic model approach for multiple precipitation reactions has been validated.
- This model was applied for identification of relevant precipitates in wastewater.
- The model described well the dynamics of competition among relevant minerals.
- Based on rates, minerals can be classified as rapidly, moderately and slow forming.

**SUPPLEMENTARY MATERIAL**

## Model validation/prediction capabilty

The following experiments were performed to test the model prediction capability using a parameter set derived on a previous data set (See manuscript) to predict performance in a new data set from a repeat experiment. The parameter values that were used are listed in Table 3 of the manuscript. The experiments carried out for this analysis were as follows:

- *Experiment 5*: this experiment was essentially a repeat of Experiment 1, but without struvite seed material added.
- *Experiment 6*: this experiment was essentially a repeat of Experiment 2 but without PO4 added.
- *Experiment 7*: this experiment was a repeat of *Experiment 3*.

The results are shown in Figures S1, S2 and S3. In general, the parameter values estimated from a different data set performed reasonably well at describing the data from the repeat experiments. Prediction of pH and dynamic state variables appeared to be qualitatively reasonable. The only instance of poor prediction appeared to be TIC in experiment 7, which was probably due to a difference between the experiments in terms of gas transfer of CO2.

***Experiment 5: Predictive performance of model with synthetic wastewater and titration***

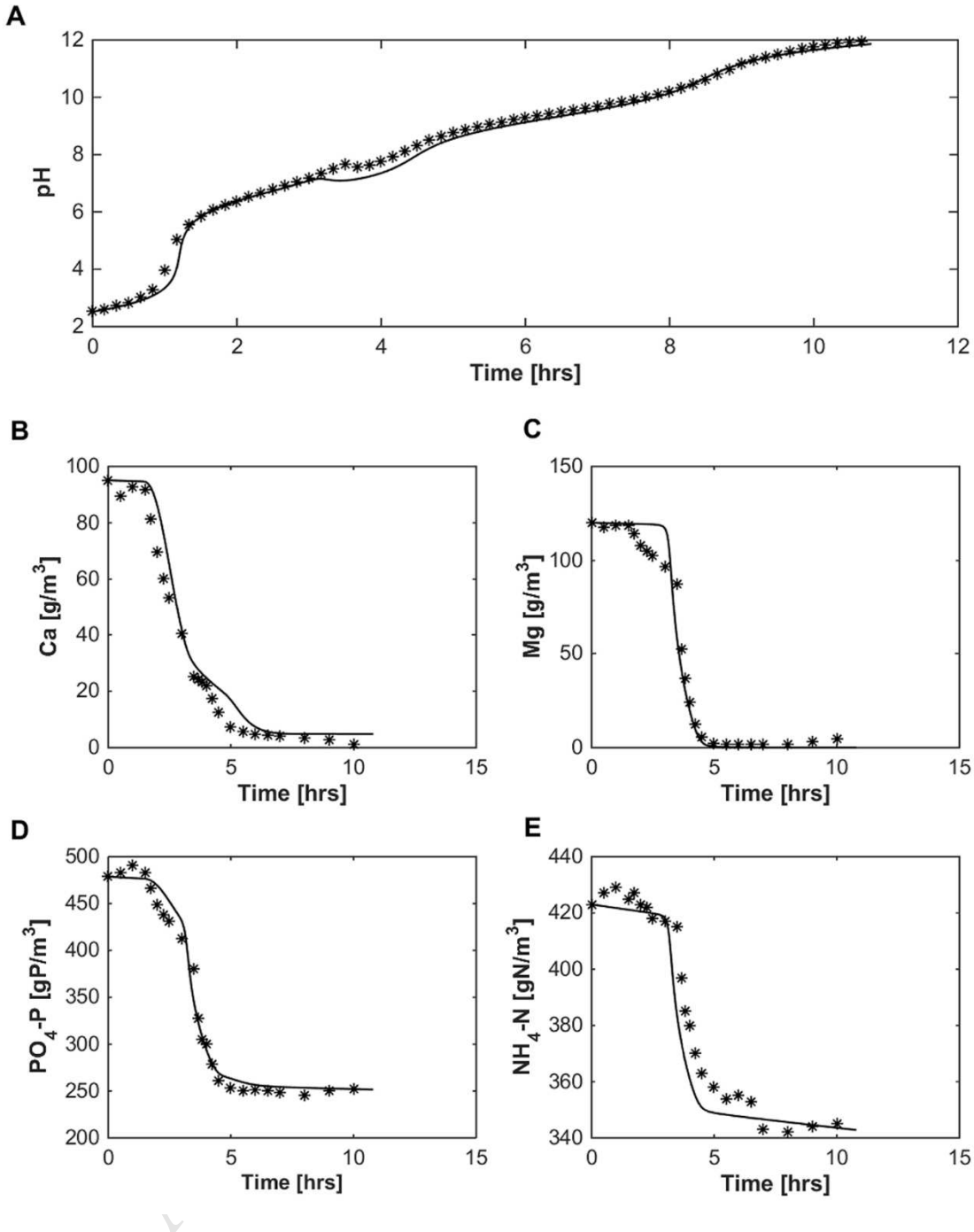


**Fig. S1 –** Experimental data vs. model prediction for *Experiment 5* with pH titration of *synthetic wastewater* with sodium hydroxide, and simulation using the optimum kinetic parameters derived from a different experiment (Experiment 1, Table 3). The symbols and the solid lines represent the experimental and simulation results, respectively.

***Experiment 6: Predictive performance of model with piggery digestate and aeration***

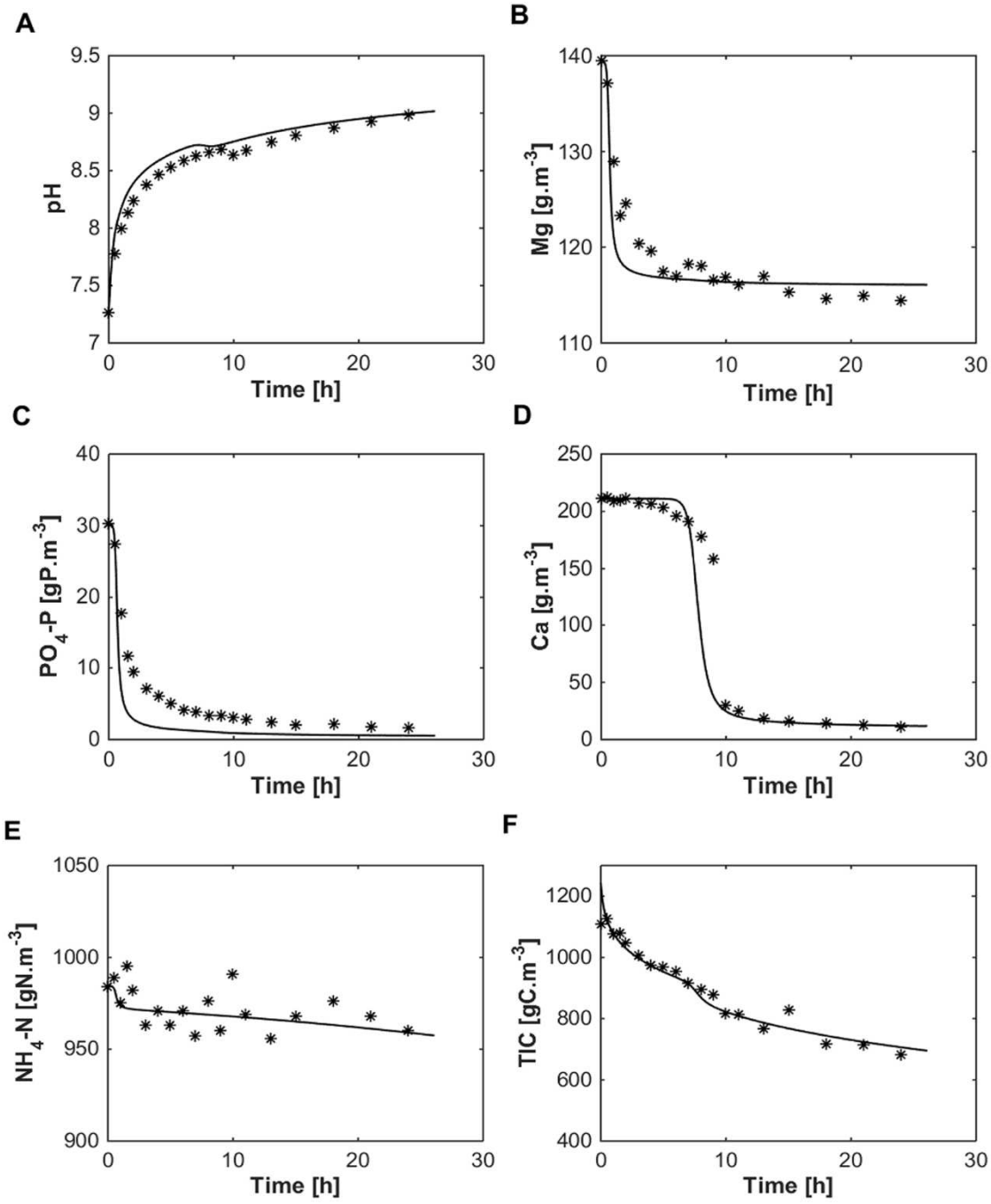


**Fig. S2 –** Experimental data vs. model prediction for *Experiment 6* with aeration of *piggery digestate* and simulation using the optimum kinetic parameters derived from a different experiment (Experiment 2, Table 3). The symbols and the solid lines represent the experimental and simulation results, respectively.

***Experiment 7: Predictive performance of model with sludge digestate and aeration***

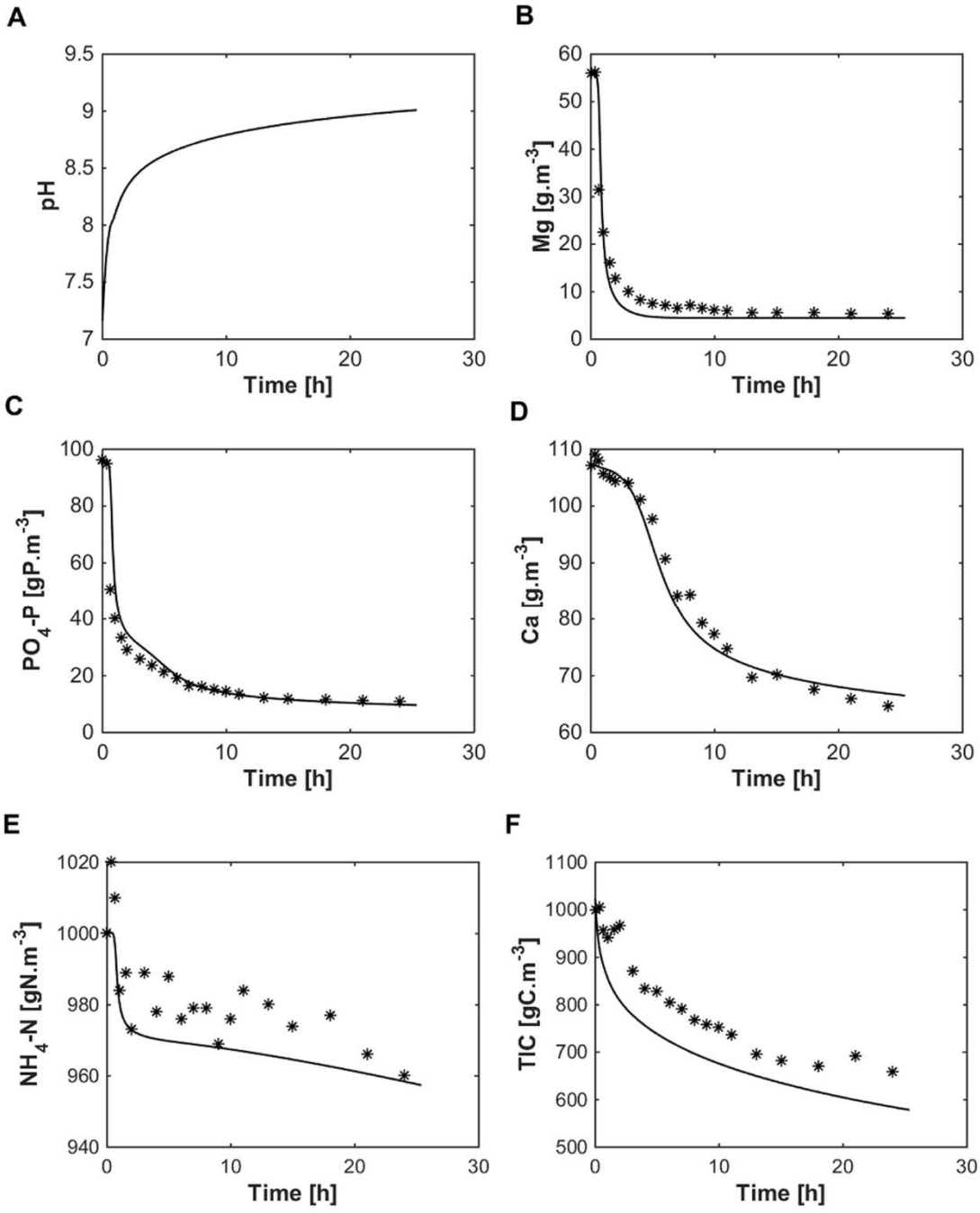


**Fig. S3** – Experimental data vs. model prediction for *Experiment 7* with aeration of *sludge digestate* and simulation using the optimum kinetic parameters derived from a different experiment (Experiment 3, Table 3). The symbols and the solid lines represent the experimental and simulation results, respectively.